

## Status of chemical equilibrium in relativistic heavy-ion collisions

J CLEYMANS

Department of Physics, University of Cape Town, Rondebosch 7701, South Africa

**Abstract.** Recent work on chemical equilibrium in heavy-ion collisions is reviewed. The energy dependence of thermal parameters is discussed. The centrality dependence of thermal parameters at SPS energies is presented.

**Keywords.** Chemical equilibrium; particle multiplicities.

**PACS Nos** 24.10.Pa; 25.75.Dw; 25.75.-q

### 1. Introduction

In hydrodynamic models [1] the freeze-out surface is very sensitive on the initial conditions and is therefore highly model dependent (see e.g. figure 1). However, this dependence disappears when considering ratios of integrated particle yields,  $N^i/N^j$ , which are independent of the details of the initial conditions and are the same as those of point-like particles in a fireball at rest,  $N_0^i/N_0^j$  [2]. If the rapidity distribution is flat (as is the case at RHIC energies) then it is furthermore possible to show that

$$\frac{dN^i/dy|_{y=0}}{dN^j/dy|_{y=0}} = \frac{N_0^i}{N_0^j}. \quad (1)$$

The conditions for the validity of these results have been discussed in the literature [2–4] and will not be repeated here.

Motivated by the above results, a systematic study of fully integrated particle multiplicities in central Au–Au and Pb–Pb collisions at beam momenta of 1.7 A·GeV, 11.6 A·GeV (Au–Au) and 158 A·GeV (Pb–Pb) has been performed [5]. The close similarity of the colliding systems makes it possible to study heavy-ion collisions under definite initial conditions over a wide range of beam energies. It can be concluded that a thermal model description of particle multiplicities, with additional strangeness suppression, is possible for each energy. The resulting temperature  $T$  and chemical potential  $\mu_B$  are shown in figure 2 which also shows results from recent fits to the RHIC data [6–8]. It can be seen that, at all energies, the average energy per hadron in the comoving frame is always close to 1 GeV per hadron despite the fact that the center-of-mass energy varies more than 100-fold [9]:

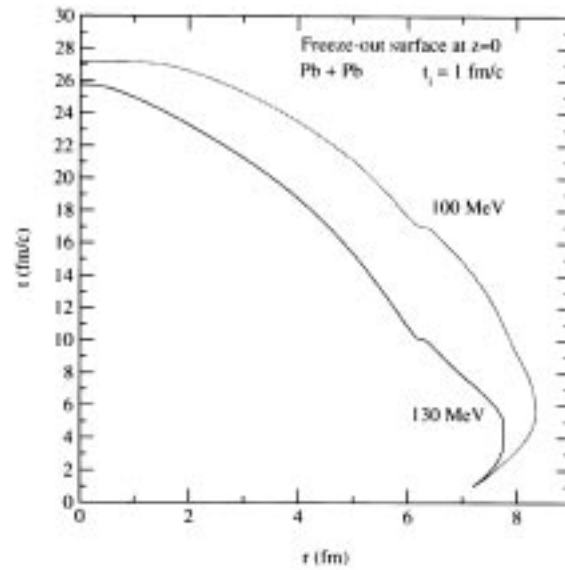


**Figure 1.** Freeze-out surface obtained in ref. [1]. The values for the thermal freeze-out temperature are indicated.

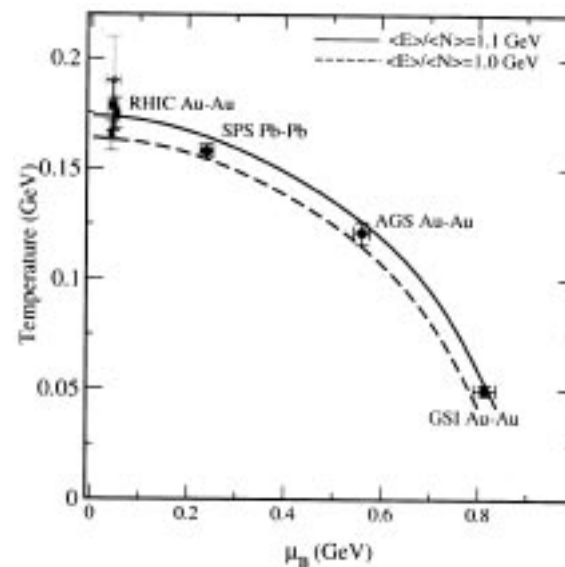


**Figure 2.** Values of thermal parameters at different energies.

$$\frac{\langle E \rangle}{\langle N \rangle} \approx 1 \text{ GeV}. \quad (2)$$

It should be noted that, with the advent of more precise data from the NA49 collaboration, this relation is now better satisfied than when it was first proposed in 1998 [9].

## 2. Energy dependence of thermal parameters

The energy dependence of the baryon chemical potential,  $\mu_B$ , can be described by a simple fit [10]

$$\mu_B(s) = \frac{a}{1 + \sqrt{s}/b} \quad (3)$$

with  $a \approx 1.27$  GeV and  $b \approx 4.3$  GeV. The temperature is then determined from eq. (2). The resulting fits to  $\mu_B(s)$  and  $T(s)$  are shown in figure 3. This parametrisation can be used to discuss the energy dependence of particle ratios. The temperature varies considerably between the lowest and the highest beam energies, namely, between 50 MeV at SIS and 160 MeV at SPS. Similarly, the baryon chemical potential changes appreciably, decreasing from about 820 MeV at SIS to about 240 MeV at SPS. The supplementary  $\gamma_s$  factor [11], measuring the deviation from a completely equilibrated hadron gas, is around 0.7–0.8 at all energies where it has been considered as a free fit parameter. At the present level of accuracy, a fully equilibrated hadron gas (i.e.  $\gamma_s = 1$ ) cannot be ruled out in all examined collisions except in Pb–Pb, where  $\gamma_s$  deviates from 1 by more than  $4\sigma$ . This result does not agree with a recent similar analysis of Pb–Pb data [12] imposing full strangeness equilibrium. The main reason for this discrepancy is to be found in the different data set used;

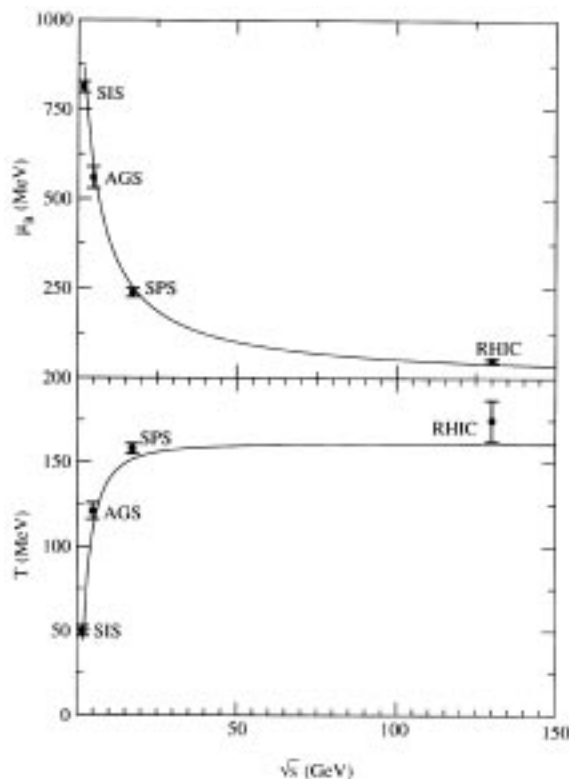


**Figure 3.** Energy dependence of the temperature and the baryochemical potential.

whilst in ref. [12] measurements in different limited rapidity intervals have been collected, we have used only particle yields extrapolated to full phase space. The temperature values that we have found essentially agree with previous analyses in Au–Au collisions [13] and estimates at 11.7 A·GeV [14].

### 3. Maximum relative strangeness

The results of the previous section combined with the energy dependence of the thermal parameters shown in figure 3 provide a basis for the study of the energy dependence of strangeness production in heavy-ion collisions. Of particular interest are the ratios of strange to non-strange particle multiplicities as well as the relative strangeness content of the system as expressed by the Wroblewski factor [15] defined as:

$$\lambda_s = \frac{2 \langle s\bar{s} \rangle}{\langle u\bar{u} \rangle + \langle d\bar{d} \rangle}. \quad (4)$$

Furthermore, we assume (for simplicity) strangeness to be in complete equilibrium, that is, the strangeness saturation factor is taken as  $\gamma_s = 1$ . When more data will become available, this point can be refined.

We turn our attention first to the energy dependence of the Wroblewski ratio. The quark content used in this ratio is determined at the moment of chemical freeze-out, i.e., from the hadrons and especially, hadronic resonances, before they decay. This ratio is thus not an easily measurable quantity unless one can reconstruct all resonances from the final-state particles. The results are shown in figure 4 as a function of invariant energy  $\sqrt{s}$ . The values calculated from the experimental data at chemical freeze-out in central A–A collisions have been taken from ref. [5]. There the statistical model was fitted with the extra parameter  $\gamma_s$  to account for the possible chemical under-saturation of strangeness. In general, values for  $\gamma_s$  close to 1 are found. At the SPS,  $\gamma_s \simeq 0.7$  gives the best agreement with  $4\pi$  data. This is also the reason why the SPS points in figure 4 lie below the solid line. The values of  $\lambda_s$  were extracted from  $4\pi$  integrated data with the exception of the result from RHIC where particle ratios were measured only at mid-rapidity [16]. The solid line in figure 4 describes the statistical model calculations in complete equilibrium along the unified freeze-out curve [9] and with the energy dependent thermal parameters presented here. From figure 4 we conclude that around 30 A·GeV lab energy, the relative strangeness content in heavy-ion collisions reaches a clear and well-pronounced maximum. The Wroblewski factor decreases towards higher incident energies and reaches a value of about 0.43.

The appearance of the maximum can be traced to the specific dependence of  $\mu_B$  on the beam energy. In figure 4 we also show the results for  $\lambda_s$  calculated under the assumption that only the temperature varies with collision energy but the baryon chemical potential is kept fixed at zero. In this case the Wroblewski factor is indeed seen to be a monotonic function of energy. The assumption of vanishing net baryon density is of course the prevailing situation in e.g.,  $p\text{--}\bar{p}$  and  $e^+e^-$  collisions. In figure 4 the results for  $\lambda_s$  extracted from the data in  $p\text{--}p$ ,  $p\text{--}\bar{p}$  and  $e^+e^-$  are also included [17]. The dashed line represents results with  $\mu_B = 0$  and a radius of 1.2 fm. There are two important differences in the behavior of  $\lambda_s$  in elementary compared to heavy-ion collisions. Firstly, the strangeness content is smaller by a factor of two. In elementary collisions, particle multiplicities follow the values given by

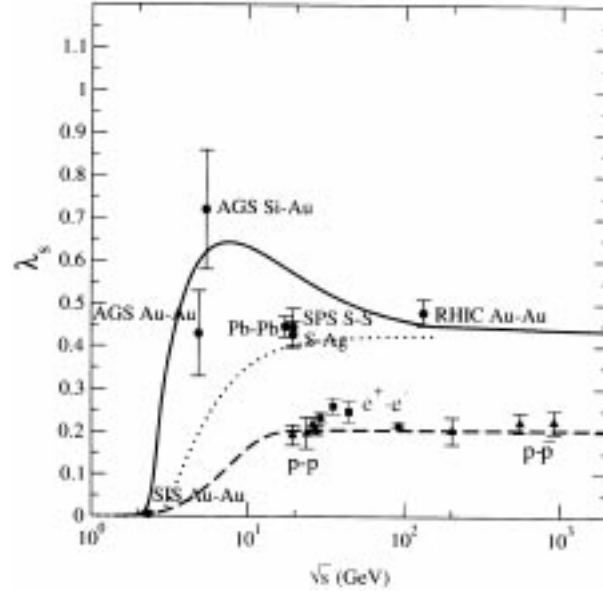


**Figure 4.** Energy dependence of the Wroblewski factor. The full line has been calculated using the energy dependence of  $T$  and  $\mu_B$  given in eq. (3) with  $\gamma_s = 1$ . The dotted line was calculated keeping  $\mu_B = 0$  and the dashed line was calculated using the canonical ensemble with a radius fixed at 1.2 fm.

the canonical ensemble with radius 1.2 fm whereas in  $A$ - $A$  collisions there is a transition from canonical to grand canonical behavior. Secondly, there is no significant maximum in the behavior of  $\lambda_s$  in elementary collisions due to the zero baryon density in the  $p$ - $\bar{p}$  and  $e^+e^-$  systems.

Following the chemical freeze-out curve, shown as a thick full line in figure 4, one can see that  $\lambda_s$  rises quickly from SIS to AGS energies, then reaches a maximum around  $\mu_B \approx 500$  MeV and  $T \approx 130$  MeV. These freeze-out parameters correspond to 30 GeV lab energy. At higher incident energies the increase in  $T$  becomes negligible but  $\mu_B$  keeps on decreasing and as a consequence  $\lambda_s$  also decreases.

The importance of finite baryon density on the behavior of  $\lambda_s$  is demonstrated in figure 4 showing separately the contributions to  $\langle s\bar{s} \rangle$  coming from strange baryons, from strange mesons and from hidden strangeness, i.e., from hadrons like  $\phi$  and  $\eta$ . As can be seen in figure 5, the origin of the maximum in the Wroblewski ratio can be traced to the contribution of strange baryons. Even strange mesons exhibit a broad maximum. This is due to the presence of associated production of e.g. kaons together with hyperons. This channel dominates at low  $\sqrt{s}$  and loses importance at high incident energies. Next we study how the behavior of the Wroblewski ratio is reflected in specific particle yields. The energy dependence of the  $\Lambda/\pi^+$  ratio is shown in figure 6. The model gives a good description of the data, showing a broad maximum at the same energy as the one seen in the Wroblewski factor. The appearance of the maximum in the relative strangeness contribution becomes also obvious when considering ratios which are more sensitive to the baryon chemical potential. Figure 6 also shows the energy dependence of the  $\Xi^-/\pi^+$  and the  $\Omega^-/\pi^+$  ratios

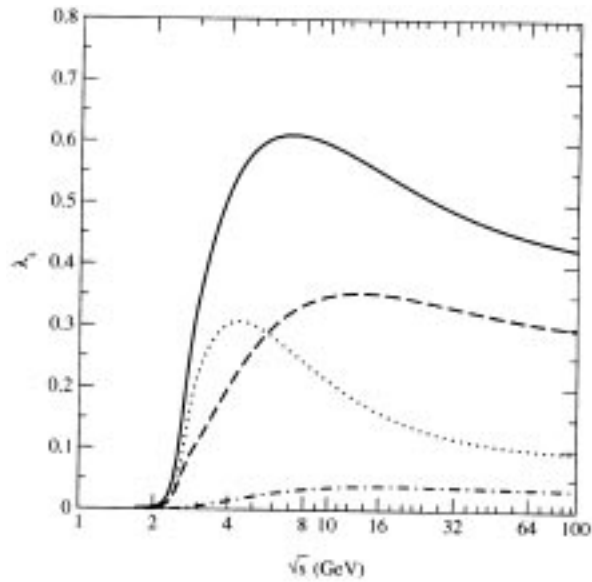


**Figure 5.** Contributions to the Wroblewski factor coming from strange baryons (dotted line), strange mesons (dashed line) and hidden strangeness (dash-dotted line).

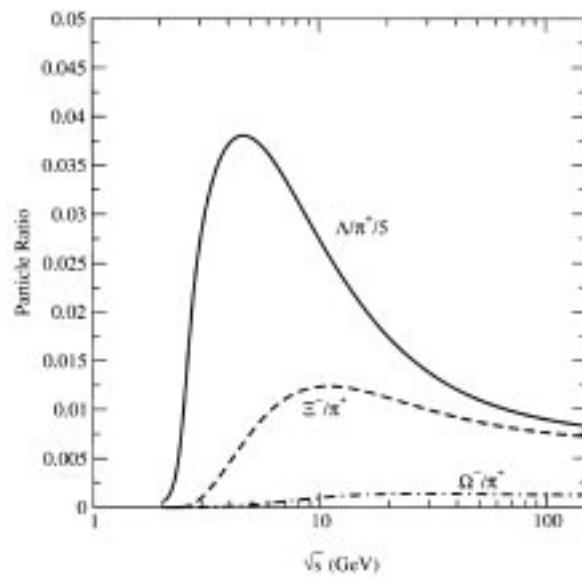


**Figure 6.** Ratios of strange baryons to pions as a function of energy for  $\gamma = 1$ .

which all exhibit maxima. The peak in the  $\Lambda/\pi^+$  ratio is much stronger than the one in the  $\Xi^-/\pi^+$  or  $\Omega^-/\pi^+$  ratios. There is also a shift of the maximum to higher energies for particles with increasing strangeness quantum number. These differences appear as a consequence of the enhanced strangeness content of the particles which suppresses the dependence of the corresponding ratio on  $\mu_B$ .

#### 4. Centrality dependence at SPS

We next analyze the centrality dependence of the thermal parameters describing hadron multiplicities [18]. This provides further information about the effects of the size of the excited strongly interacting system and help in the systematic understanding of the experimental data. We will show that the thermal model is able to describe the available data for various centrality classes at one beam energy.

In order to have a sound basis for the application of the thermal model, we rely as much as possible on fully integrated particle multiplicities. For this reason we concentrate our efforts on the analysis of results obtained by the NA49 collaboration [19] using centrality selected fixed-target Pb–Pb collisions at a beam energy of 158 GeV per nucleon, which are analyzed here within the framework of the thermal model.

As shown in [5], the inclusion or omission of certain hadron species can change the extracted values of  $T$  and  $\mu_B$  considerably. We stress however that our analysis, due to the restricted available data, focuses on the trends with changing centrality. The temperature,  $T$ , and the baryon chemical potential,  $\mu_B$ , do not show any noticeable dependence on centrality [18]. There are two thermal parameters which exhibit a pronounced dependence on centrality: the strangeness equilibration factor  $\gamma_s$  increases approximately linearly and saturates for increasing centrality, as shown in figure 7. Other thermodynamic state variables, such as the energy per hadron  $\langle E \rangle / \langle N \rangle$ , the energy density, the baryon density and the entropy per baryon  $S/B$ , remain fairly independent of the centrality.

In summary, the analysis of the thermal parameters, describing the integrated yields of  $\pi^\pm$ ,  $K^\pm$  and  $\bar{p}$  as obtained by the NA49 experiment [19] shows that the radius of the fireball increases linearly with increasing centrality. Also the strangeness parameter  $\gamma_s$  increases, i.e., strange particle multiplicities approach chemical equilibrium. In contrast,

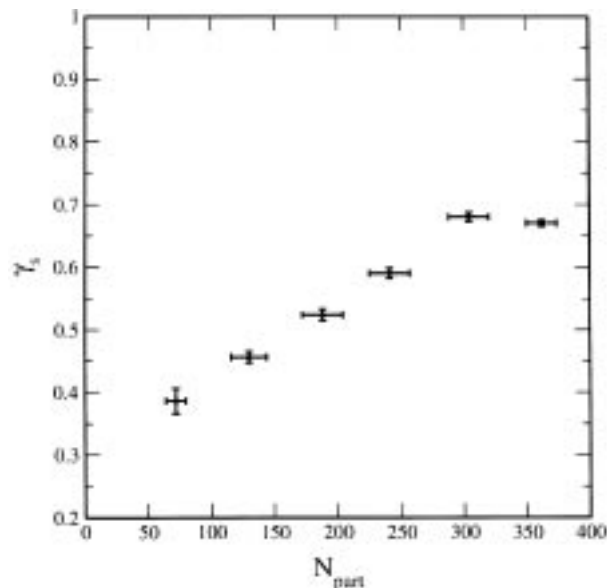


Figure 7. Centrality dependence of the strangeness suppression factor  $\gamma_s$ .

the temperature and the baryon chemical potential do not change with centrality. No in-medium modifications are needed to describe the above quoted hadron yields.

### Acknowledgements

Helpful discussions with H Oeschler, K Redlich, F Becattini, A Keränen, E Suhonen, B Kaempfer, P Braun-Munzinger, J Stachel, S Wheaton, S Yacoob and M Marais are acknowledged. Thanks are also due to D Röhrich, P Seyboth and R Stock for invaluable help with the NA49 data.

### References

- [1] J Cleymans, K Redlich and D K Srivastava, *Phys. Rev.* **C55**, 1431 (1997)
- [2] J Cleymans and K Redlich, *Phys. Rev.* **C60**, 054908 (1999)
- [3] D H Rischke, *Proc. 15th Int. Conf. on Ultra-relativistic Nucleus–Nucleus Collisions (QM2001)* (Stony Brook, New York) 15–20 January 2001  
Lecture Notes in Physics 516, *Hadrons in dense matter and hadrosynthesis* edited by J Cleymans, H B Geyer and F G Scholtz (Springer-Verlag, 1999)
- [4] U Heinz, *Nucl. Phys.* **A661**, 140c (1999)
- [5] F Becattini, J Cleymans, A Keränen, E Suhonen and K Redlich, *Phys. Rev.* **C64**, 024901 (2001)
- [6] N Xu, *Proc. 15th Int. Conf. on Ultra-Relativistic Nucleus–Nucleus Collisions (QM2001)* (Stony Brook, New York) 15–20 January 2001; nucl-ex/0104021 *Nucl. Phys. A* (in print)
- [7] P Braun-Munzinger, D J Magestro, K Redlich and J Stachel, hep-ph/0105223
- [8] W Florkowski, W Broniowski and M Michalec, nucl-th/0106009
- [9] J Cleymans and K Redlich, *Phys. Rev. Lett.* **81**, 5284 (1998)
- [10] P Braun-Munzinger, J Cleymans, H Oeschler and K Redlich, *Nucl. Phys. A* (to be published) (2001)
- [11] J Letessier, J Rafelski and A Tounsi, *Phys. Rev.* **C50**, 406 (1994)  
C Slotta, J Sollfrank and U Heinz, *Proc. Strangeness in Hadronic Matter* edited by J Rafelski (AIP Press, Woodbury, 1995) p. 462
- [12] P Braun-Munzinger, I Heppel and J Stachel, *Phys. Lett.* **B465**, 15 (1999)
- [13] J Cleymans, H Oeschler and K Redlich, *Phys. Rev.* **C59**, 1663 (1999) and references therein
- [14] J Stachel, *Nucl. Phys.* **A610**, 509c (1996)
- [15] A Wroblewski, *Acta Phys. Pol.* **B16**, 379 (1985)
- [16] J Harris, STAR Collaboration, *Proc. 15th Int. Conf. on Ultra-relativistic Nucleus–Nucleus Collisions (QM2001)* (Stony Brook, New York) 15–20 January 2001; *Nucl. Phys. A* (in print) (2001)
- [17] F Becattini, Lecture Notes in Physics 516, *Hadrons in dense matter and hadrosynthesis* edited by J Cleymans, H B Geyer and F G Scholtz (Springer-Verlag, 1999)
- [18] J Cleymans, B Kaempfer and S Wheaton, *Phys. Rev. C* (to be published) (2001)
- [19] F Sikler, for the NA49 Collaboration, *Nucl. Phys.* **A661**, 45c (1999)